Tri-level lung cancer classification via deep learning based GoogleNet with computed tomography images

Vinoth Rathinam[1], Ramathilagam Arunagiri[2], Valarmathi Krishnasamy[1], Sasireka Rajendran[3]
[1]Department of Electronics and Communication Engineering, P.S.R. Engineering College, Sivakasi, India
[2]Department of Computer Science and Engineering, P.S.R. Engineering College, Sivakasi, India
[3]Department of Biotechnology, Mepco Schlenk Engineering College, Sivakasi, India

Article Info

Article history:

Received Sep 4, 2024
Revised Nov 30, 2024
Accepted Dec 25, 2024

Keywords:

Computed tomography images
Gaussian star filter
GoogleNet
Lung cancer
Support vector machine

ABSTRACT

Lung cancer (LC) is one of the most prevalent causes of cancer-related death worldwide. World Health Organization (WHO) classifies LC into two broad histological subtypes: non-small cell lung cancer (NSCLC) which is the cause of about 85% of cases and small cell lung cancer (SCLC) which makes up the remaining 15%. Several issues can influence LC detection including poor image quality, insufficient training data, low-quality image characteristics, and poor tumor localization. To overcome these challenges a novel TRI-level LC classification via deep learning-based GoogleNet with computed tomography (CT) images (TRI-LCNet) approach has been proposed for early-stage LC detection using CT images. Initially, the LC-input images CT are collected from openly accessible datasets. The lung CT images have been preprocessed using a Gaussian star filter (GaSF) to decrease noise, followed by feature extraction using GoogleNet. The extracted LC features are then given into a support vector machine (SVM) which is utilized as a classification tool to distinguish between different classes of LC cases. The TRI-LCNet approach performance was assessed by several metrics: specificity, accuracy, F1 score, and recall. The outcomes show that the suggested method obtains a higher accuracy range of 96.93% for the early identification of LC.

Corresponding Author:

Vinoth Rathinam
Department of Electronics and Communication Engineering, P.S.R. Engineering College
Sivakasi-626140, Tamilnadu, India
Email: vinoth@psr.edu.in

1. INTRODUCTION

Lung cancer (LC) afflicts both men and women and accounts for nearly 25% of all cancer-related fatalities [1]. Roughly 80% of deaths from causes of LC directly by smoking. LC primarily occurs in two forms: non-small cell lung cancer (NSCLC), the most common, and small cell lung cancer (SCLC) [2]. Accordingly, it is predicted that of 30,000 Canadians in 2020, 21,000 will receive an LC diagnosis and will lose their lives to the illness. By 2050, the frequency of LC globally is expected to have doubled, making it the most common cancer. Air pollution, diesel exhaust, asbestos exposure at work, secondhand smoke, radon exposure, and other factors can cause LC in non-smokers or other substances some people do not smoke [3]. Various diagnostic procedures, containing X-rays, CT scans, biopsies, and sputum cytology, are conducted to detect malignant cells and rule out other conditions. Skilled pathologists evaluate the microscopic histopathology slides obtained during biopsies to diagnose LC and identify its subtypes [4], [5]. Numerous types of LC are difficult for pathologists and other medical professionals to diagnose quickly [6]. Misdiagnosis of cancer types is rising, leading to unsuitable treatments and potential patient death. Machine learning (ML) is a branch of AI, that makes computers learn from data and improve tasks through experience [7], [8]. Low-dose CT (LDCT) is an effective LC screening method, demonstrating 85% selectivity and 99% specificity in the NELSON trial [9]. A recent investigation found an overall false positive rate of 81% [10], necessitating further imaging for validation [11]. Numerous public and private LC databases support early detection strategies. A multi-model network architecture accommodates varying nodule sizes, reducing training time [12]. This approach achieves 90.6% accuracy using ensemble learning for lung nodule classification [13], [14], providing an LC detection network.

Recent studies have investigated various lung cancer detection (LCD) frameworks, primarily utilizing ML approaches [15]. Hatuwal and Thapa [16] highlighted the effectiveness of convolutional neural networks (CNNs), achieving accuracy rates of 96.2% for validation and 96.11% for training. Shah *et al.* [17] improved detection accuracy using ensemble methods, reaching a total accuracy of 95%. Venkatesh *et al*. [18] used optimized CNNs, achieving 96.97% accuracy while reducing false positives. Naseer *et al*. [19] employed AlexNet, reporting specificity, sensitivity, and accuracy rates of 96.77%, 99.08%, and 97.64%, respectively. Shanthi and Rajkumar [20] proposed a wrapper-based feature selection algorithm employing a modified stochastic diffusion search (SDS), demonstrating superior performance. Mridha *et al.* [21] identified specific protein markers for early detection, complementing ML methods. Rehman *et al.* [22] reported 91% and 93% accuracy rates with K-nearest neighbors and support vector machine (SVM) classifiers, while Patra [23] introduced a radial basis function (RBF) classifier with 81.25% accuracy. Mathios *et al.* [24] presented a non-invasive method using cell-free DNA fragmentomes, achieving a 94% detection rate via CT imaging. Lastly, Li *et al.* [25] addressed challenges in LDCT and emphasized its role in reducing LC mortality through early detection. Several challenges have been identified in existing methods for detecting LC including poor image quality, insufficient training data, inaccurate tumor localization, and difficulty in reducing false positives. Additionally, existing models such as CNN and RBF classifiers exhibit lower accuracy, and non-invasive methods require further refinement for clinical use. A novel TRI-level lung cancer classification via deep learning-based GoogleNet with CT images (TRI-LCNet) approach has been proposed for early-stage LCD utilizing CT images to overcome these issues. The primary contributions of the research are as follows:

- The primary objective of this research is to develop a novel TRI-LCNet approach for early-stage LC detection.
- Initially, the lung CT images are pre-processed utilizing a Gaussian star filter (GaSF) to reduce the noise and improve clarity for more accurate analysis.
- The preprocessed CT images of the lungs are obtained as input for GoogleNet to extract the significant features.
- The images are used for the following phase by concatenating the extracted features using SVM to classify cases of normal, NSCLC, and SCLC.
- The efficacy of the proposed TRI-LCNet was measured utilizing performance metrics namely precision, recall, accuracy, F1 score, and specificity.

The remainder of this research has been scheduled as follows. The full explanation of the proposed TRI-LCNet method for LC detection is in section 2. Results and discussion in section 3 and a conclusion and future work in section 4.

2. METHOD

In this section, a novel TRI-LCNet has been proposed for detecting different classes of LC such as normal, SCLC, and NSCLC. The overall workflow of the suggested TRI-LCNet approach is portrayed in Figure 1.

2.1. Dataset description

The lung image database consortium and image database resource initiative (LIDC-IDRI) dataset comprise LC screening thoracic CT images and diagnostics from 1,018 patients. It includes over 1,000 annotated lesions by four experienced radiologists, capturing both nodules and non-nodule findings. The scans come with metadata describing patient demographics, lesion characteristics, and malignancy likelihood. The dataset is widely used for research in LCD tasks.

2.2. Data pre-processing

The medical images are enhanced by pre-processing, which reduces noise and enhances subtle changes. Initially, the LC-input CT images were preprocessed using GaSF to enhance the features of the image by lessening noise and enhancing the visibility of lung structures, which can aid in more accurate feature extraction.

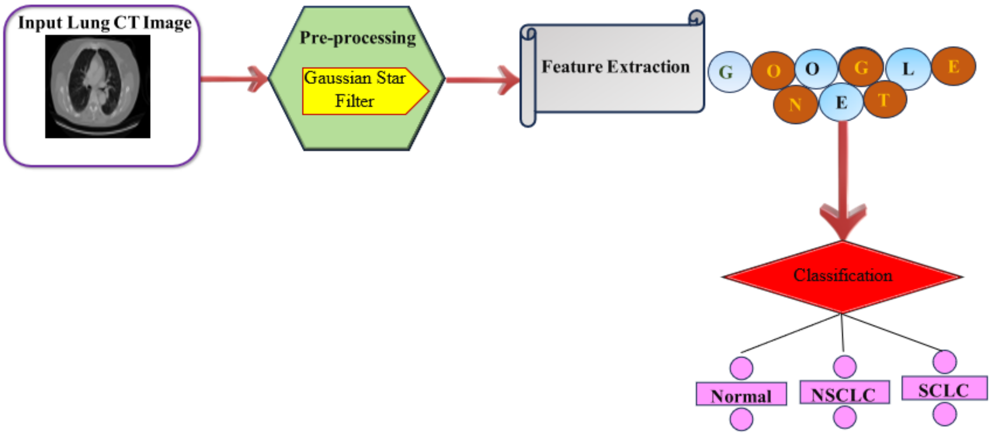

Figure 1. The overall workflow of the TRI-LCNet framework

2.2.1. Gaussian star filter

GaSF enhances lung CT scans by highlighting star-like structures, correlating with pathological features, and reducing noise while preserving important details, particularly star shapes. The Mathematical expression of the proposed Gaussian star low pass filter is as (1):

$$GaSLF(u,v) = \begin{cases} GSaLF_{(u,v)} = \begin{cases} \max(H_1, H_2) if\ H_1 \neq 0 \\ H_1 + H_2\ else \end{cases} & \text{if GaSLF } (u,v) = 0 \\ GaSLF_{(u,v)} = GaSLF(u,v)\ else \end{cases} \quad (1)$$

Where u_n, v_n are the n^{th} peak point center points of the filter, and a_n and b_n are calculated using a region-growing technique with ellipse parameters.

$$H_1(u,v) = \sum_{N=1}^{N} e^{\frac{-D_{1n}{}^2(u,v)}{2}} \quad (2)$$

$$D_{1n}(u,v) = \left(\frac{u-u_n}{a_n}\right)^2 + \left(\frac{v-v_n}{b_n}\right)^2 \quad (3)$$

$$H_2(u,v) = \sum_{n=1}^{N} e^{\frac{-D_{2n^2(u,v)}}{2}} \quad (4)$$

$$D_{2n}(u,v) = \left(\frac{u-u_n}{b_n}\right)^2 + \left(\frac{v-v_n}{a_n}\right)^2 \quad (5)$$

Finally, in the frequency system, the proposed GaSF, is defined as (6):

$$GSF(u,v) = 1 - GaSLF(u,v) \quad (6)$$

The values of the GaSLF coefficients range from 1 to 0. The GaSF estimated parameter design aims to eliminate noise zones identified within the image. Additionally, GaSF is suggested for filtering gray-level images tainted by periodic or quasi-periodic noise.

2.3. Feature extraction

Lung image features are extracted and analyzed by first gathering a substantial amount of raw data, which is then divided into manageable cohorts. GoogleNet simplifies this process by extracting high-and low-level features from pre-processed lung CT images through its deep architecture and inception modules.

2.3.1. GoogleNet

One kind of construction uses a neural network with convolution and the inception architecture is called GoogleNet. The network may select from each block range of convolutional filter sizes thanks to the use of inception modules. An inception network arranges these modules in a stack on top of one another, occasionally utilizing stride 2 max-pooling layers, the grid resolution can be cut in half. The GoogleNet inception module architecture is demonstrated in Figure 2.

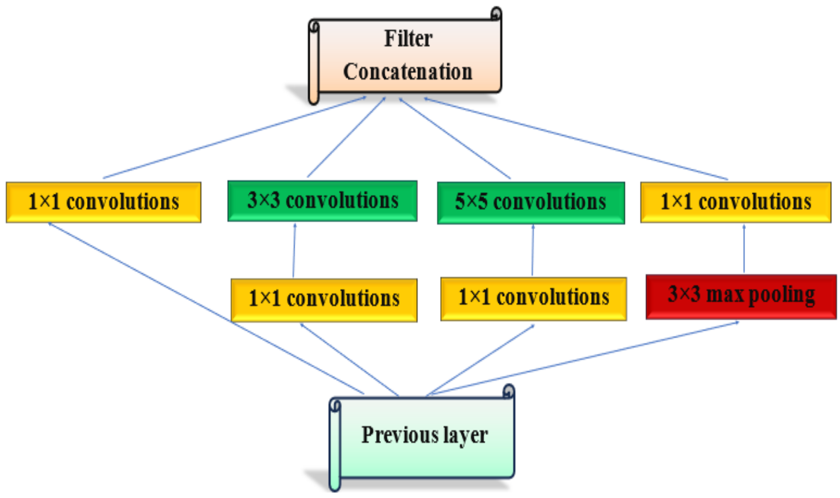

Figure 2. The architecture of the GoogleNet inception module

In contrast to earlier cutting-edge architectures like AlexNet and ZF-Net, the GoogleNet architecture is significantly different. It creates deeper architecture by utilizing a variety of techniques, including global average pooling and 1×1 convolution. A simple mathematical representation of an inception module, let's assume three types of operations (1×1, 3×3, and 5×5 convolutions) are performed, and their outputs are concatenated:

$$Inception = Concat\left(Conv_{1x1}(X), Conv_{3x3}(X), Conv_{5\times 5}(X), Pool(X)\right) \quad (7)$$

where X is the input to the inception module, and Concat denotes the concatenation of feature maps along the channel dimension. Its efficient design with reduced parameters and innovative use of 1x1 convolutions makes it an effective tool for image categorization tasks.

2.4. Support vector machine

An ML under supervision approach for applications involving regression and classification is the SVM. For its efficiency in elevated dimensions' areas and its capacity for categorization difficulties, it is very well-liked to create decision boundaries that maximize the margin between different classes. The mathematical representation of SVM finds a hyperplane in a dataset that is linearly separable defined by:

$$w.x + b = 0 \quad (8)$$

Here, w represents the weight vector, b denotes the bias and x represents the input feature vector. The hyperplane is subject to the following constraint for correctly classified data points:

$$y_{i(w.x_i+b)} \geq 1 \quad (9)$$

where y_i is the class label $(+1\ or - 1)$ for each data point x_i. This constraint ensures that the data points are correctly classified with the maximum margin from the hyperplane. For datasets that are linearly not separable, SVM employs kernel functions to project the data into a high-dimension space, in which a linear hyperplane is utilized to separate the classes. The decision function for SVM can be represented as (10):

$$f(x) = sign(\sum_{i=1}^{N} \propto_i y_i K(x_i, x) + b) \quad (10)$$

Here, $K(x_i, x)$ denotes the kernel function that determines the likeness between both data points x_i and x, and $\propto_i$ are the Lagrange multipliers obtained from the optimization problem.

2.4.1. Non-small cell lung cancer

NSCLC constitutes 85% of LCs, primarily linked to smoking, air pollution, genetics, asbestos, or radon exposure. Symptoms include chronic cough, chest pain, dyspnea, weight loss, and fatigue. Prognosis hinges on early detection, and treatment response, and advancements in targeted therapies and immunotherapy have enhanced outcomes, aided by mathematical models predicting tumor growth and treatment efficacy.

$$N(t) = N_0 . e^{rt} \tag{11}$$

Where $N(t)$ indicates the count of tumor cells with time t, N_0 denotes the starting cell count, while r denotes the growth rate. Tumor growth that slows down as the tumor reaches a larger size:

$$N(t) = N_0 . e^{\frac{k}{r}} . (1 - e^{-rt}) \tag{12}$$

where K is the carrying capacity of the environment, and r is the initial growth rate.

2.4.2. Small cell lung cancer

SCLC is closely linked to smoking and spreads rapidly, with key risk factors including secondhand smoke, radiation, asbestos, and genetics. It presents symptoms like chronic cough, chest pain, dyspnea, fatigue, and edema, and is staged as limited or extended based on its spread. Treatment options include chemotherapy, radiation, and immunotherapy, while mathematical models predict tumor growth and pharmacokinetic models assess how drugs are absorbed, metabolized, and eliminated in the body.

$$C(t) = \frac{D.k_a}{V_d(K_a - K_e)} . \left(e^{-k_e t} - e^{-k_a t}\right) \tag{13}$$

where the quantity of medication present at time t is indicated by C(t), D is the administered dose, k_a is the rate constant of absorption, k_e is the constant of the elimination rate and v_d is the distribution volume.

3. RESULTS AND DISCUSSION

The LIDC-IDRI dataset is utilized in this subsection to assess the performance of the TRI-LCNet. The CT images are sourced from the LIDC-IDRI dataset and pre-processed into appropriate frames before being further processed. To estimate findings, the test samples were analyzed using accuracy, specificity, precision, f1score, and recall.

Figure 3 displays the visualization of the TRI-LCNet approach using the LIDC-IDRI dataset. Column 1 shows the input with raw lung CT scan images, followed by column 2, where the images are pre-processed using a GaSF to enhance quality by reducing noise and improving clarity. In column 3, GoogleNet is employed for feature extraction, focusing on the critical features needed for accurate classification. Finally, column 4 presents the results, effectively distinguishing between Normal, NSCLC, and SCLC.

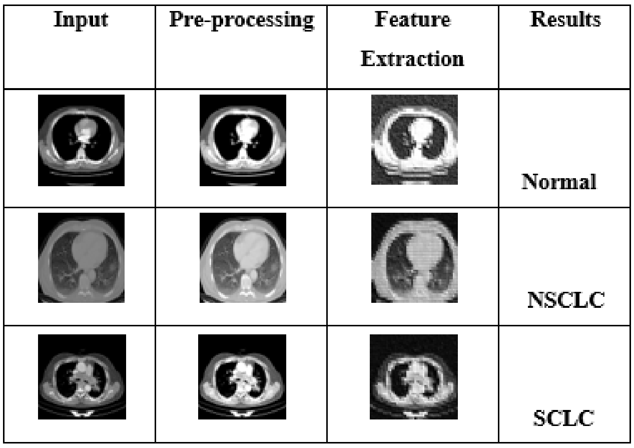

Figure 3. Experimental results of proposed TRI-LCNet

3.1. Performance analysis

Specificity, recall, accuracy, precision, and F1 score are the factors for evaluation that will be applied to gauge the effectiveness of the planned LCD network. Where T_{pos} and T_{neg} indicate the actual benefits and drawbacks of the sample images, F_{pos} and F_{neg} shows the sample images false positives and negatives.

$$Specificity = \frac{T_{neg}}{T_{neg}+F_{pos}} \tag{14}$$

$$Precision = \frac{T_{pos}}{T_{pos}+F_{pos}} \tag{15}$$

$$Recall = \frac{T_{pos}}{T_{pos}+F_{neg}} \tag{16}$$

$$Accuracy = \frac{T_{pos}+T_{neg}}{Total\ no.of\ samples} \tag{17}$$

$$F1\ score = 2\left(\frac{Precision*Recall}{Precision+Recall}\right) \tag{18}$$

Table 1 illustrates the efficiency assessment of the TRI-LCNet across three classes namely Normal, NSCLC, and SCLC. For the normal class, the model delivered 97.12% specificity, 98.24% precision, 96.25% recall, a 96.69% F1 score, and 98.41% accuracy. In NSCLC, TRI-LCNet achieved 94.27% specificity, 96.12% precision, 95.05% recall, a 95.48% F1 score, and 97.25% accuracy. For SCLC, it obtained 96.24% specificity, 97.28% precision, 96.08% recall, a 96.52% F1 score, and 95.13% accuracy. A graphic representation of the suggested TRI-LCNet performance evaluation is provided in Figure 4.

Table 1. Performance analysis of the TRI-LCNet approach

Classes	Specificity	Precision	Recall	Accuracy	F1 score
Normal	97.12	98.24	96.25	98.41	96.69
NSCLC	94.27	96.12	95.05	97.25	95.48
SCLC	96.24	97.28	96.08	95.13	96.52

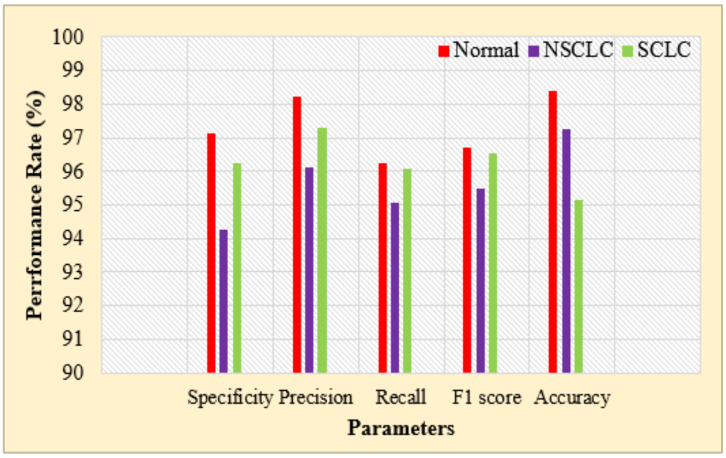

Figure 4. A graphic representation of the performance analysis for several LC classes

The accuracy graph in Figure 5 is estimated using the accuracy range and 100 epochs. As the number of epochs rises, the accuracy also rises. Figure 6 displays the loss range, showing that the loss decreases with increasing epochs. The suggested approach achieves an outstanding level of LCD accuracy by utilizing CT images. The results showed that the suggested has a low error rate and a 96.93% classification accuracy based on 100 training epochs.

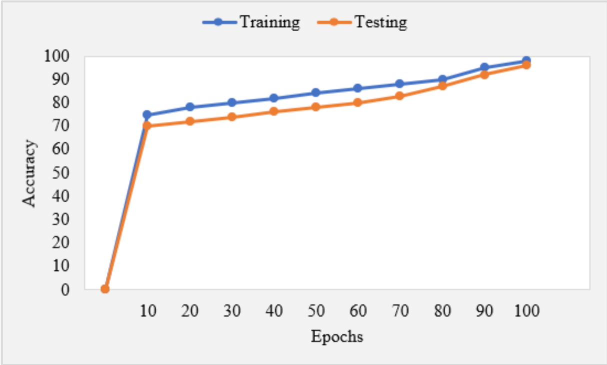

Figure 5. Accuracy curve of the suggested TRI-LCNet

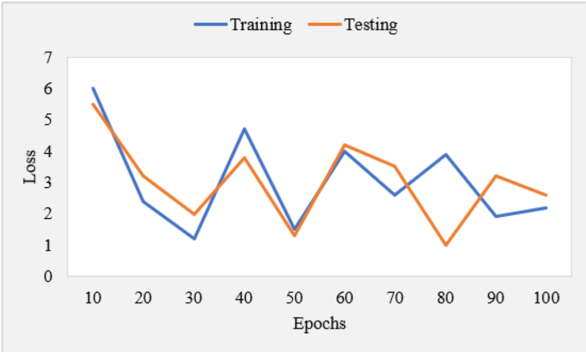

Figure 6. Loss curve of the suggested TRI-LCNet

3.2. Comparative analysis

The efficacy of every network was estimated to confirm that the outcomes of the TRI-LCNet achieve high accuracy. The proposed GoogleNet with four DL classifiers LeNet, VGG-16, AlexNet, and the proposed TRI-LCNet Model was tested for competency. The comparison of various feature extraction is demonstrated in Table 2. The suggested GoogleNet achieves 97.6% accuracy than AlexNet, LeNet, and VGG-16 which obtains 6.55%, 8.29%, and 5.22%. A range of criteria were used to estimate each network's performance, including specificity, recall, precision, F1 score, and accuracy.

Table 2. Comparison of several networks and proposed network

Networks	Specificity	F1 score	Precision	Recall	Accuracy
AlexNet	89.2	86.0	87.5	84.6	91.2
LeNet	88.7	85.7	86.2	85.3	89.5
VGG-16	90.6	88.8	89.0	88.7	92.5
GoogleNet	97.8	94.4	98.4	96.5	97.6

Table 3 demonstrates the accuracy comparison between prior approaches and the suggested TRI-LCNet for LC detection. The TRI-LCNet approach enhances the accuracy of 0.75%, 6.41%, 16.17%, and 4.05% better than CNN, SDS, RBF, and ML. This demonstrates TRI-LCNet's superior performance in LC detection compared to several traditional frameworks.

Table 3. Accuracy comparison of state-of-art models and proposed TRI-LCNet

Authors	Methods	Accuracy (%)
Hatuwal and Thapa [16]	CNN	96.2
Shanthi and Rajkumar [20]	SDS	90.71
Rehman *et al.* [22]	ML	93
Patra [23]	RBF	81.25
Proposed	TRI-LCNet	96.93

The performance assessment of the proposed TRI-LCNet model using various lung CT image datasets, including LIDC-IDRI, LUNA16, NSCLC radiogenomics, and Cohen's lc, is shown in Table 4. The TRI-LCNet model demonstrates the highest accuracy (96.93%) and F1 score (96.23%) on the LIDC-IDRI dataset, which is likely due to the detailed annotations of lung nodules in this dataset. The LUNA16 dataset also shows a strong efficiency of 95.02% accuracy and a 93.51% F1 score. However, the model's performance declines slightly on the NSCLC radiogenomics and Cohen's lc datasets, which may be attributed to differences in dataset structure and variability in the features used. Despite this, the TRI-LCNet model maintains a high level of efficiency across all datasets, highlighting its robustness for LCD tasks.

Table 4. Efficiency analysis of the TRI-LCNet model with different datasets

Datasets	Accuracy	F1 score
LIDC-IDRI (ours)	96.93	96.23
LUNA16	95.02	93.51
NSCLC radiogenomics	92.68	90.25
Cohen's lung cancer	94.23	92.56

3.3. Discussion

In this work, the TRI-LCNet model was developed for detecting and classifying LC types such as normal, NSCLC, and SCLC using CT images from the LIDC-IDRI dataset. The results demonstrate significant improvements in accuracy and efficiency over existing models. The suggested GoogleNet achieved an overall accuracy of 97.6%, outperforming AlexNet, LeNet, and VGG-16 with accuracy improvements of 6.55%, 8.29%, and 5.22% respectively, as shown in Table 2. Additionally, TRI-LCNet outperformed other prior methods with an accuracy improvement of 0.75% over CNN and up to 16.17% over RBF classifiers, as illustrated in Table 3. The model's performance across different datasets detailed in Table 4 shows that TRI-LCNet achieved the highest accuracy on the LIDC-IDRI dataset (96.93%) and strong performance on LUNA16 (95.02%). Although there was a slight performance decline on the NSCLC Radiogenomics and Cohen's LC datasets, TRI-LCNet still maintained a high level of efficiency, highlighting its robustness for LCD tasks. Figures 5 and 6 illustrate the steady rise in accuracy and lower loss across the epochs, confirming the model's generalization capability. Overall, the TRI-LCNet model provides a highly accurate and efficient solution for early LCD, significantly decreasing false positives and offering a promising tool for improving patient outcomes.

3.4. Clinical setting

The clinical integration of the proposed TRI-LCNet model is designed for the efficient classification of LC cases employing CT images applicable in hospital settings. The system involves patients undergoing diagnosis and treatment with their lung CT images being collected. These images are processed by the TRI-LCNet model which classifies the cases into normal, NSCLC, or SCLC categories. The results are then provided to doctors assisting them in refining the patient's diagnosis and treatment plan. The real-time clinical application of the TRI-LCNet model can be tested in radiology departments and diagnostic centers to verify its accuracy in detecting LC. Furthermore, this system could be integrated into telemedicine platforms for remote diagnosis, and it can be evaluated across various hospitals in clinical trials to assess its performance in diverse patient populations. Such practical applications demonstrate the robustness of the TRI-LCNet model and its potential to enhance the early detection and treatment of LC increasing patient outcomes in real-world healthcare environments.

4. CONCLUSION

In this work, a novel TRI-LCNet approach has been proposed for early-stage LCD. Initially, the LC-input images CT are collected from the datasets that are openly accessible. The lung CT images have been preprocessed using a GaSF to decrease noise, followed by feature extraction using GoogleNet. The extracted LC features are then concatenated and fed into an SVM which is used as a classification tool to distinguish between different classes of LC cases. The LC detection performance network performance involved applying a few metrics, including recall, F1 score, specificity, accuracy, and precision measurements. The outcomes of the experiment show that the TRI-LCNet framework offers a high accuracy range of 96.93% for early detection of LC. The proposed TRI-LCNet is limited by its reliance on a small dataset, affecting generalizability, and the scalability of SVM may hinder performance with larger, high-dimensional data. Future work could involve expanding the dataset for better generalizability and integrating multimodal data such as clinical factors to further enhance diagnostic accuracy.

ACKNOWLEDGMENTS
The authors would like to thank the management for their constant support.

FUNDING INFORMATION
Authors state no funding was received.

AUTHOR CONTRIBUTIONS STATEMENT
This journal uses the Contributor Roles Taxonomy (CRediT) to recognize individual author contributions, reduce authorship disputes, and facilitate collaboration.

Name of Author	C	M	So	Va	Fo	I	R	D	O	E	Vi	Su	P	Fu
Vinoth Rathinam	✓	✓	✓	✓	✓	✓		✓	✓	✓				
Ramathilagam Arunagiri		✓		✓		✓				✓	✓			
Valarmathi Krishnasamy	✓		✓	✓		✓				✓	✓	✓		
Sasireka Rajendran	✓	✓	✓	✓	✓	✓		✓	✓	✓				

C : **C**onceptualization
M : **M**ethodology
So : **So**ftware
Va : **Va**lidation
Fo : **Fo**rmal analysis
I : **I**nvestigation
R : **R**esources
D : **D**ata Curation
O : Writing - **O**riginal Draft
E : Writing - Review & **E**diting
Vi : **Vi**sualization
Su : **Su**pervision
P : **P**roject administration
Fu : **Fu**nding acquisition

CONFLICT OF INTEREST STATEMENT
Authors state no conflict of interest.

INFORMED CONSENT
We have obtained informed consent from all individuals included in this study.

ETHICAL APPROVAL
This study did not require ethical approval as it involved only publicly available data, which was analyzed anonymously and did not involve any identifiable human subjects.

DATA AVAILABILITY
Data availability is not applicable to this paper as no new data were created or analyzed in this study.

REFERENCES

[1] R. Nooreldeen and H. Bach, "Current and future development in lung cancer diagnosis," *International Journal of Molecular Sciences*, vol. 22, no. 16, pp. 1–18, Aug. 2021, doi: 10.3390/ijms22168661.
[2] R. S. K. Boddu, P. Karmakar, A. Bhaumik, V. K. Nassa, Vandana, and S. Bhattacharya, "Analyzing the impact of machine learning and artificial intelligence and its effect on management of lung cancer detection in covid-19 pandemic," *Materials Today: Proceedings*, vol. 56, pp. 2213–2216, 2022, doi: 10.1016/j.matpr.2021.11.549.
[3] N. S. Reddy and V. Khanaa, "Intelligent deep learning algorithm for lung cancer detection and classification," *Bulletin of Electrical Engineering and Informatics*, vol. 12, no. 3, pp. 1747–1754, Jun. 2023, doi: 10.11591/eei.v12i3.4579.
[4] Y. Chen, J. Feng, J. Liu, B. Pang, D. Cao, and C. Li, "Detection and Classification of Lung Cancer Cells Using Swin Transformer," *Journal of Cancer Therapy*, vol. 13, no. 07, pp. 464–475, 2022, doi: 10.4236/jct.2022.137041.
[5] A. Heidari, D. Javaheri, S. Toumaj, N. J. Navimipour, M. Rezaei, and M. Unal, "A new lung cancer detection method based on the chest CT images using Federated Learning and blockchain systems," *Artificial Intelligence in Medicine*, vol. 141, Jul. 2023, doi: 10.1016/j.artmed.2023.102572.
[6] G. S. Saragih, Z. Rustam, and J. E. Aurelia, "A hybrid model based on convolutional neural networks and fuzzy kernel K-medoids for lung cancer detection," *Indonesian Journal of Electrical Engineering and Computer Science*, vol. 24, no. 1, pp. 1–8, Oct. 2021, doi: 10.11591/ijeecs.v24.i1.pp126-133.
[7] S. G. Ortiz, R. H. Ortiz, A. J. Gavilanes, R. Á. Faican, and B. P. Zambrano, "A serial image analysis architecture with positron emission tomography using machine learning combined for the detection of lung cancer," *Revista Española de Medicina Nuclear e Imagen Molecular (English Edition)*, vol. 43, no. 3, May 2024, doi: 10.1016/j.remnie.2024.500003.

[8] S. Wankhade and S. Vigneshwari, “A novel hybrid deep learning method for early detection of lung cancer using neural networks,” *Healthcare Analytics*, vol. 3, pp. 1–13, Nov. 2023, doi: 10.1016/j.health.2023.100195.
[9] W. Chiangjong *et al.*, “Cell-main spectra profile screening technique in simulation of circulating tumour cells using maldi-tof mass spectrometry,” *Cancers*, vol. 13, no. 15, pp. 1–15, Jul. 2021, doi: 10.3390/cancers13153775.
[10] S. R. Quasar, R. Sharma, A. Mittal, M. Sharma, D. Agarwal, and I. de La T. Díez, “Ensemble methods for computed tomography scan images to improve lung cancer detection and classification,” *Multimedia Tools and Applications*, vol. 83, no. 17, pp. 52867–52897, Nov. 2024, doi: 10.1007/s11042-023-17616-8.
[11] M. S. Bhuiyan *et al.*, “Advancements in Early Detection of Lung Cancer in Public Health: A Comprehensive Study Utilizing Machine Learning Algorithms and Predictive Models,” *Journal of Computer Science and Technology Studies*, vol. 6, no. 1, pp. 113–121, Jan. 2024, doi: 10.32996/jcsts.2024.6.1.12.
[12] T. I. A. Mohamed, O. N. Oyelade, and A. E. Ezugwu, “Automatic detection and classification of lung cancer CT scans based on deep learning and ebola optimization search algorithm,” *PLoS ONE*, vol. 18, no. 8, Aug. 2023, doi: 10.1371/journal.pone.0285796.
[13] G. Chassagnon *et al.*, “Artificial intelligence in lung cancer: current applications and perspectives,” *Japanese Journal of Radiology*, vol. 41, no. 3, pp. 235–244, Nov. 2023, doi: 10.1007/s11604-022-01359-x.
[14] C. Abbosh *et al.*, “Tracking early lung cancer metastatic dissemination in TRACERx using ctDNA,” *Nature*, vol. 616, no. 7957, pp. 553–562, Apr. 2023, doi: 10.1038/s41586-023-05776-4.
[15] S. G. Armato *et al.*, “The Lung Image Database Consortium (LIDC) and Image Database Resource Initiative (IDRI): A completed reference database of lung nodules on CT scans,” *Medical Physics*, vol. 38, no. 2, pp. 915–931, Feb. 2011, doi: 10.1118/1.3528204.
[16] B. K. Hatuwal and H. C. Thapa, “Lung Cancer Detection Using Convolutional Neural Network on Histopathological Images,” *International Journal of Computer Trends & Technology*, vol. 68, no. 10, pp. 21–24, Oct. 2020, doi: 10.14445/22312803/ijctt-v68i10p104.
[17] A. A. Shah, H. A. M. Malik, A. H. Muhammad, A. Alourani, and Z. A. Butt, “Deep learning ensemble 2D CNN approach towards the detection of lung cancer,” *Scientific Reports*, vol. 13, no. 1, pp. 1–15, Feb. 2023, doi: 10.1038/s41598-023-29656-z.
[18] C. Venkatesh, K. Ramana, S. Y. Lakkisetty, S. S. Band, S. Agarwal, and A. Mosavi, “A Neural Network and Optimization Based Lung Cancer Detection System in CT Images,” *Frontiers in Public Health*, vol. 10, pp. 1–9, Jun. 2022, doi: 10.3389/fpubh.2022.769692.
[19] I. Naseer, T. Masood, S. Akram, A. Jaffar, M. Rashid, and M. A. Iqbal, “Lung Cancer Detection Using Modified AlexNet Architecture and Support Vector Machine,” *Computers, Materials and Continua*, vol. 74, no. 1, pp. 2039–2054, 2023, doi: 10.32604/cmc.2023.032927.
[20] S. Shanthi and N. Rajkumar, “Lung Cancer Prediction Using Stochastic Diffusion Search (SDS) Based Feature Selection and Machine Learning Methods,” *Neural Processing Letters*, vol. 53, no. 4, pp. 2617–2630. 2021, doi: 10.1007/s11063-020-10192-0.
[21] M. F. Mridha *et al.*, “A Comprehensive Survey on the Progress, Process, and Challenges of Lung Cancer Detection and Classification,” *Journal of Healthcare Engineering*, pp. 1–43, Dec. 2022, doi: 10.1155/2022/5905230.
[22] A. Rehman, M. Kashif, I. Abunadi, and N. Ayesha, “Lung Cancer Detection and Classification from Chest CT Scans Using Machine Learning Techniques,” in *2021 1st International Conference on Artificial Intelligence and Data Analytics (CAIDA)*, IEEE, Apr. 2021, pp. 101–104. doi: 10.1109/CAIDA51941.2021.9425269.
[23] R. Patra, “Prediction of lung cancer using machine learning classifier,” in *Computing Science, Communication and Security: First International Conference, COMS2 2020*, Gujarat, 2020, India, pp. 132-142, doi: 10.1007/978-981-15-6648-6_11.
[24] D. Mathios *et al.*, “Detection and characterization of lung cancer using cell-free DNA fragmentomes,” *Nature Communications*, vol. 12, no. 1, pp. 1–14, Aug. 2021, doi: 10.1038/s41467-021-24994-w.
[25] C. Li *et al.*, “Advances in lung cancer screening and early detection,” *Cancer Biology and Medicine*, vol. 19, no. 5, pp. 591–608, May 2022, doi: 10.20892/j.issn.2095-3941.2021.0690.

BIOGRAPHIES OF AUTHORS

Vinoth Rathinam received his Bachelors of Engineering–Electronics and Communication Engineering from Mohamed Sathak Engineering College and Master of Engineering in VLSI Design under Anna University in the year 2007 and 2009 respectively. He received his Ph.D. in Information and Communication Engineering under Anna University in the year 2017. His area of interest includes image processing, signal processing, and VLSI design. He has more than 15 years of professional experience in Engineering Colleges. He has received grant of Rs.3.5lakhs for organizing AICTE ATAL FDP during 2023-24. He can be contacted at email: vinoth@psr.edu.in.

Ramathilagam Arunagiri is working as a Professor in the Department of Computer Science and Engineering at P.S.R. Engineering College, Sivakasi. She has 21 years of teaching experience. She completed her Ph.D. in Information and Communication Engineering from Anna University in the year 2018. She obtained her M.E. Computer Science, Engineering in the year 2004, B.E. Computer Science, and Engineering in the year 1999 from Arulmigu Kalasalingam College of Engineering, Krishnankovil. She has published 15 papers in reputed international/national journals and presented 20 papers in National and International conferences. Her research interests are computer network, security, cloud computing, big data analytics, machine learning, and data science. She can be contacted at email: ramathilagam@psr.edu.in.

Valarmathi Krishnasamy is currently working as a Professor in the Department of Electronics and Communication Engineering at P.S.R. Engineering College, Sivakasi, Tamil Nadu, India. She is having 25 years of teaching experience. She has published 46 papers in peer reviewed international journals and presented 84 papers in various national and international conferences. She has received best paper award for her paper in the International Conference on VLSI communication and Instrumentation (ICVCI 2011). Her research interests are system identification, image processing, soft computing, wireless networks, cloud computing, and machine learning. She can be contacted at email: valarmathi@psr.edu.in.

Sasireka Rajendran received her B.Tech. Biotechnology from Kumaraguru College of Technology and Master of Technology in Biotechnology from Mepco Schlenk Engineering College under Anna University in the year 2012 and 2014 respectively. Currently she is pursuing Ph.D. under Anna University, Chennai. She has cleared Graduate Aptitude Test in Engineering. She obtained university 6th Rank during her Post Graduate programme. She also received Summer Faculty Research Fellowship at IIT Delhi and Indian Academy of Sciences Summer Fellowship at IIT Guwahati in the year 2015 and 2016 respectively. Her area of interest includes cancer biology and enzyme technology. She can be contacted at email: sasirekabt@mepcoeng.ac.in.